Available online at www.sciencedirect.com

ScienceDirect

Acta Materialia 78 (2014) 236–244

Acta MATERIALIA

www.elsevier.com/locate/actamat

Stability and mobility of screw dislocations in 4H, 2H and 3C silicon carbide

L. Pizzagalli

Institut P', CNRS UPR 3346, Université de Poitiers, SP2MI, BP 30179, Boulevard Marie et Pierre Curie, 86962 Futuroscope Chasseneuil Cedex, France

Received 16 May 2014; received in revised form 18 June 2014; accepted 21 June 2014

Abstract

Large-scale first-principles calculations were performed to determine the stability and mobility properties of screw dislocations in common silicon carbide polytypes (4H, 2H and 3C). There is a profound lack of knowledge regarding these dislocations, although experimental observations show that they govern the plastic behavior of SiC at low temperature. Numerical simulations reported in this paper indicate that these dislocations are characterized by a shuffle core, the associated Peierls stress of which ranges from 8.9 to 9.6 GPa depending on the polytype. The only other stable dislocation core exhibits a reconstruction along the dislocation line, with a greater stability, but is also found to be sessile. Polytypism has a weak influence on these results, especially regarding dislocation core energies and Peierls stress. However, a qualitative difference is predicted between the cubic and the hexagonal systems regarding slip planes, with a possible dislocation displacement along a prismatic plane on average, which would result from a zigzag motion of the screw dislocations at the atomic scale.

Keywords: Silicon carbide; Sislocations; Plasticity

1. Introduction

Silicon carbide exhibits an impressive list of interesting properties, many of which are already exploited in different domains [1]. Some of these properties follow from the very high stability of this compound. Hence, SiC is a ceramic with high strength and large hardness, and exhibits excellent behavior in extreme temperature environments (high thermal shock resistance, low thermal expansion, high thermal conductivity, low fracture toughness). Consequently, it is then used in many applications, such as abrasive and cutting tools, and automobile brakes. Besides these outstanding mechanical properties, SiC is also highly resistant to irradiation, which makes this material a first-choice candidate for various nuclear applications, such as a structural material in future fusion reactors [2,3] and as a fuel cladding material in next-generation fission reactors. SiC has also a low chemical reactivity with a good resistance to corrosion, and thus has potential application in harsh environments. Considering its electronic properties, SiC is a semiconductor that can be doped, like silicon. It is also characterized by a large gap, and a high value of the critical electric field. SiC is therefore used in high-power high-temperature devices. The combination of all these electrical, mechanical and thermal properties makes SiC an interesting material for biosensor applications [4].

Nevertheless, the use of SiC in certain applications is limited by the difficulty of growing high-quality SiC crystals, with a controlled quantity of residual defects such as dislocations, although great improvements have been achieved in recent years. These dislocations, for instance, limit the potential of SiC in electronic and electromechanical applications. Knowledge of the characteristics of dislocations is therefore important for achieving a better control

E-mail address: Laurent.Pizzagalli@univ-poitiers.fr

http://dx.doi.org/10.1016/j.actamat.2014.06.053
1359-6454/

of their formation depending on the conditions. Furthermore, determining the properties of dislocations is essential for improving our current understanding of the mechanical behavior of silicon carbide (for a review, see e.g. Ref. [5]). In the ductile regime, at high temperature, dislocations in SiC are dissociated, like in silicon. These partial dislocations have been the focus of several dedicated studies [6–14]. At room temperature, it has been recently revealed that dislocations are non-dissociated screw [15], and require large stresses to move. The transition between these two regimes is not sharp, with the coexistence of both dissociated and non-dissociated dislocations over a large temperature range [16,17]. Unlike partial dislocations, there have been very few investigations of the properties of non-dissociated screw dislocations [18,19], resulting in a serious lack of information. For instance, the most stable core for a non-dissociated screw dislocation in silicon, which exhibits a double-period reconstruction along the dislocation line [20,21], has not been considered as a possible option for SiC. Furthermore, the Peierls stress of the non-dissociated screw dislocation is not known. With recent experimental developments enabling the mechanical properties of materials to be studied at a small scale, for which very high yield stresses are observed [22], it becomes increasingly important to achieve a complete determination of dislocation properties.

An additional issue associated with SiC is polytypism, with several competing phases. Among the 250 different identified polytypes [1], the most common ones are the hexagonal 4H, 6H and the cubic 3C. The structures of these phases essentially differ by the stacking of atomic layers along the $\langle 0001\rangle$ ($\langle 111\rangle$) direction for hexagonal (cubic) polytypes. An important feature of polytypes is that their local atomic environments are similar up to the second-neighbor shell. It is often assumed, therefore, that the properties of defects do not depend much on polytypism. This is why, for instance, most theoretical investigations of point and extended defects have been based on 3C-SiC, although experimental data are usually obtained using hexagonal polytypes. To our knowledge, this assumption has never been verified in the case of dislocations.

This paper reports the results of investigations aiming at addressing some of the issues described above. First-principles calculations have been performed to study the structure and stability of various possible core configurations for a non-dissociated screw dislocation in 3C-, 2H- and 4H-SiC. The Peierls stress has been computed for the stable configurations, and the differences between cubic and hexagonal polytypes are discussed.

2. Models and simulation setup

The calculations were performed in the framework of density functional theory [31,32], using the PWscf package of the Quantum Espresso project [33]. In this work, exchange and correlation contributions were obtained using the now-standard generalized gradient approximation functional proposed by Perdew, Burke and Ernzerhof (GGA-PBE) [34]. Only contributions from valence electrons were explicitly computed by employing ultrasoft pseudopotentials [35]. A plane-wave energy cutoff of 30 Ry (160 Ry) for the wavefunctions (charge density) was found to be a good compromise between accuracy and computational resources.

The validity of this computational framework was assessed by comparing calculated lattice parameters and elastic constants (using small systems and large k-point sets) to reference values (Table 1). An excellent agreement is obtained for lattice parameters, with values slightly overestimated by at most 1%. Considering elastic constants, single-crystal measurements are only available for 4H [25] and 3C [26] polytypes, and our results compare extremely well to these data.

Three-dimensional periodic boundary conditions were employed here, since they are particularly appropriate to plane-wave-based density functional theory calculations. Oblique computational cells, as initially proposed by Bigger et al. [36], were selected, enabling the generation of a quadrupolar array of dislocations while containing only two dislocations with Burger vectors of opposite sign. This framework was shown to be the most suited for modeling screw dislocations, with minimal elastic interactions [37,38]. Fig. 1 shows the relevant orientations [39]. For hexagonal polytypes 2H and 4H, corresponding unitary vectors are $\hat{x} = \frac{1}{\sqrt{2}}[1\bar{1}00], \hat{y} = [0001]$ and $\hat{z} = \frac{1}{\sqrt{2}}[11\bar{2}0]$, while for cubic 3C, $\hat{x} = \frac{1}{\sqrt{6}}[1\bar{1}21], \hat{y} = \frac{1}{\sqrt{3}}[111]$ and $\hat{z} = \frac{1}{\sqrt{2}}[10\bar{1}]$.

Table 1
Lattice constant a (Å), c/a ratio, and elasticity constants (GPa) computed in this work for 2H, 4H and 3C-SiC, and compared to experimental [23–27] and DFT data [28–30].

	This work	[23]	[24]	[28]	
	2H				
a	3.0885	3.079	3.0763	3.05	
c/a	1.6460	1.641	1.641	1.64	
C_{11}	499			541	
C_{12}	93			117	
C_{13}	52			61	
C_{33}	533			586	
C_{44}	153			162	
	This work	[25]	[24]	[29]	
	4H				
a	3.0903		3.073	3.087	
c/a	3.2936		3.271	3.254	
C_{11}	498	501		534	
C_{12}	91	111		96	
C_{13}	52	52		50	
C_{33}	535	553		574	
C_{44}	159	163		171	
	This work	[24]	[26]	[27]	[30]
	3C				
a	4.3804	4.3596			4.344
C_{11}	382		395	390	390
C_{12}	128		123	142	134
C_{44}	239		236	256	253

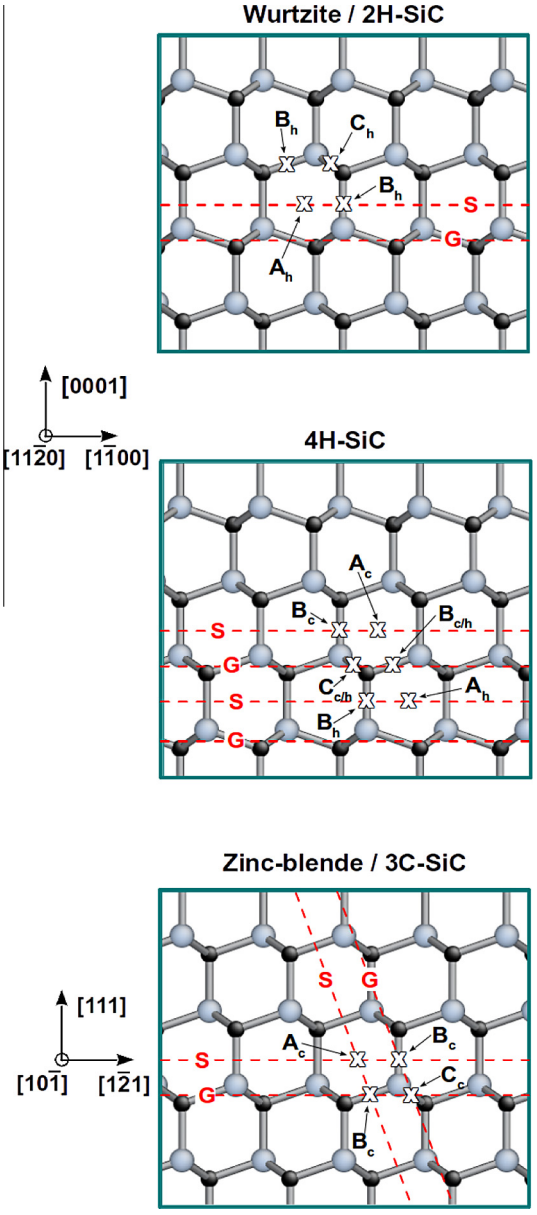

Fig. 1. Ball-and-stick representation of the 2H (wurtzite), 4H and 3C (zinc-blende) SiC structures considered in this work, projected along pertinent orientations for dislocations, [11$\bar{2}$0] for hexagonal and [10$\bar{1}$] cubic polytypes. White crosses show possible locations for screw dislocation cores, while dashed red lines indicate "shuffle" (S) and "glide" (G) basal and {111} planes for hexagonal and cubic systems, respectively (color for online version). (For interpretation of the references to colour in this figure caption, the reader is referred to the web version of this article.)

The screw dislocation line is then oriented along $\hat{z}$. In the case of 2H-SiC, the computational cell vectors are $\vec{u} = 8\sqrt{3a}\hat{x}, \vec{v} = 4\sqrt{3a}\hat{x} + 4c\hat{y} + a/2\hat{z}$ and $\vec{w} = 2a\hat{z}$ (considering a and c as provided by Table 1), thus including 512 atoms. Equivalent cells are obtained for 4H-SiC using cell vectors $\vec{u} = 8\sqrt{3a}\hat{x}, \vec{v} = 4\sqrt{3a}\hat{x} + 2c\hat{y} + a/2\hat{z}$, and $\vec{w} = 2a\hat{z}$. Finally, in the case of 3C-SiC, cell vectors are $\vec{u} = 4\sqrt{6a}\hat{x}, \vec{v} = 2\sqrt{6a}\hat{x} + 3\sqrt{3a}\hat{y} + \sqrt{2a}/4\hat{z}$ and $\vec{w} = \sqrt{2a}\hat{z}$, encompassing 576 atoms. Note that the small $\hat{z}$ component of the $\vec{v}$ vector is needed in the case of screw dislocations, to prevent lattice mismatch at the cell boundaries [37].

Because of their long-range elastic field, the two dislocations contained in the computational cell interact with each other, as well as with replicated dislocations because of periodic boundary conditions. As long as these interactions can be fully described by the linear elasticity theory, it is quite easy to extract properties associated with a single dislocation. In this work, cell dimensions were large compared to previous similar calculations, allowing for a separation of at least 20.33 Å between two dislocations. This is certainly big enough to employ the linear elasticity theory framework. The large dimensions along $\hat{x}$ and $\hat{y}$ also suggest that the Brillouin zone sampling can be accurately achieved by using two k-points distributed along $\hat{z}$ [40].

The determination of Peierls stresses for all stable cores was done by first applying an increasing shear strain on the computational cell. The critical shear strain was then calculated as the threshold value for which the dislocation is displaced from one Peierls valley to the next. Close to this value, strain increments as low as 0.1% were employed for an accurate determination. The Peierls stress was finally obtained by multiplying the critical shear strain by the corresponding elastic modulus. The latter can be computed from the computed elastic constants reported in Table 1. However, this is based on the assumption that the elastic response of the system to the shear is linear, which might be erroneous for large strain values. Another method is to apply an equivalent shear strain on a pristine bulk system of similar dimension, and compute the excess energy. The elastic modulus C can then be determined by matching this quantity with the elastic energy stored into the system $\frac{1}{2}C\varepsilon^2$. For Peierls stress determinations of single-period dislocation cores, the previously described computational cell was halved along the dislocation line to lower the computational cost. However, an almost equivalent accuracy was achieved by considering four special k-points along the $\hat{z}$ axis.

3. Structure and stability of possible dislocation cores

Fig. 1 shows the three SiC polytypes investigated in this study, oriented along relevant directions for dislocation modeling. Depending on the position of the dislocation line in (11$\bar{2}$0) (hexagonal) or (10$\bar{1}$) (cubic) planes, different core structures can be obtained by relaxing initial atomic displacements yielded by anisotropic elasticity theory. These positions, labeled as different letters A, B and C in Fig. 1, are the center of (1) an hexagon and (2) a "long" or (3) a "short" bond (as seen when projected on the planes mentioned above). Although it is possible to initially put the dislocation center in other locations, the latter moves to A or C during structural relaxation with first-principles or empirical force fields in any cases. This point appears to

be valid for zinc-blende and wurtzite materials investigated in earlier studies [18,41,42,19,43]. Here, in addition, one has to consider possible differences due to the hexagonal or cubic local character of the structure. For instance, there are two inequivalent A_c and A_h positions for 4H-SiC (Fig. 1).

The A core has been suggested as a possible non-dissociated screw dislocation structure in the pioneering work of Hornstra [44] since the separations between the dislocation center and first-neighbor atoms are maximized, thus minimizing the lattice distortions associated with the defect. In this configuration, the dislocation is located in the "shuffle" set of {111} (cubic) or basal (hexagonal) layers [45]. The A core has been found to be stable in various zinc-blende [46–48] and wurtzite [43] materials. In this work, the stability of A_h and A_c dislocation cores was confirmed for 2H-, 4H- and 3C-SiC.

An example of a relaxed A_c structure is shown in Fig. 2. The analysis of the atomic displacements reveals an increase of 2–6% of the length of "long" bonds in the hexagon encircling the dislocation center. These bonds are also characterized by a tilt of 0.6–0.7 Å along $\hat{z}$ (the dislocation line direction) due to the dislocation. For hexagonal "short" bonds, the situation is more complex. In fact, the presence of the dislocation breaks the symmetry, leading to alternating longer (+10%) and shorter (−5%) bonds. The former are also characterized by an increase of the original $\hat{z}$ tilt by about 0.18 Å, while a decrease of similar extent is obtained for the latter. A careful examination of A_c (in 3C and 4H) and A_h (in 4H and 2H) configurations show that the polytype has negligible influence on the geometries of dislocation cores.

In the reference textbook by Hirth and Lothe [39] the B core is reported as an alternative configuration. However, all previous first-principles calculations in silicon unambiguously showed that it is not stable [42,19]. Celli had early hinted at this instability on the basis of a symmetry argument [49], although it is not clear whether the latter is still relevant in the case of a binary compound such as SiC. In this study, three B cores were tested (B_c for 3C-SiC, B_h for 2H-SiC, and $B_{c/h}$ for 4H-SiC). In all cases, they were found to be unstable and relaxing to the A configuration. This emphasizes an issue related to several empirical potentials, which are not able to reproduce this result [43,50,18].

The last case corresponds to the dislocation center in the C position, in the "glide" set of {111} (cubic) or basal (hexagonal) layers [45]. Previous investigations have shown that first-principles or interatomic potential relaxation starting from elasticity theory positions lead to the formation of a sp^2 hybridized dislocation core for 3C-SiC [18,19], called the C core here. However, in the present study, it is found that a sp^3 hybridized C_2 core is recovered during relaxation for all polytypes (C_c for 3C, C_h for 2H, and $C_{c/h}$ for 4H), through the formation of Si–Si and C–C bonds along the dislocation line (Fig. 2). This configuration has been identified as the most stable one in silicon [20]. Starting from a sp^2 core structure initially relaxed using interatomic potentials yields the same outcome. Then it appears that a simple period C core is not stable in SiC. The results of previous calculations can be understood if one considers that the computation cells employed in these works were restricted to a single layer along $\hat{z}$, artificially preventing the C_2 core formation. Finally, an intermediate configuration C_2^* was tested for 2H and 3C, in which these C–C bonds are initially present but not the Si–Si bonds. In both cases, the fully reconstructed C_2 core was recovered during relaxation. As mentioned above, the main structural feature of the C_2 dislocation core is the formation of Si–Si and C–C bonds oriented along the dislocation line. Silicon bonds have a bond length of 2.49–2.52 Å depending on the polytype, i.e. an increase of about 7% compared to bulk silicon. Carbon bonds are 5% larger than in diamond, with lengths of 1.62–1.64 Å. As for the A dislocation core, a potential influence of the polytype on the C_2 core geometry is too small to be estimated.

The computed energy differences between the only two stable core structures, A and C_2, clearly show that C_2 is

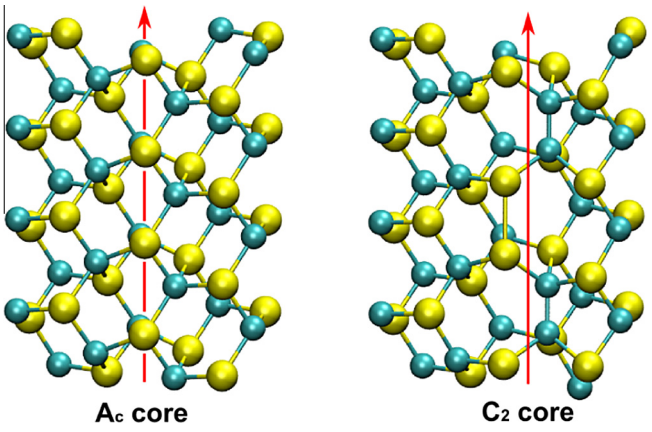

Fig. 2. Ball-and-stick representation of the two stable cores, A_c (left) and C_2 (right), for a non-dissociated screw dislocation in 3C-SiC. The red lines mark the position of the dislocation line ([111] orientation). (For interpretation of the references to colour in this figure caption, the reader is referred to the web version of this article.)

Table 2
Energy differences (in eV Å^{-1}) relative to the most stable one (C_2 for all polytypes), dislocation core radii (in Å) and energies (in eV Å^{-1}) for different screw dislocation configurations (see Fig. 1 or text for configuration labels). Arrows indicate unstable configurations while blank fields correspond to non-tested cases.The dislocation core energies are determined by assuming that r_c is equal to the Burgers vector (see text for explanations).

	2H	4H	3C
	Excess energy differences (eV Å^{-1})		
A	0.148	0.146	0.152
B	→ A	→ A	→ A
C	→ C_2	→ C_2	→ C_2
C_2^*	→ C_2		→ C_2
C_2	**0**	**0**	**0**
	r_c (Å) / E_C (eV Å^{-1})		
A	0.78 / 1.15	0.82 / 1.13	0.73 / 1.20
C_2	0.93 / 1.00	0.98 / 0.98	0.87 / 1.05

the most stable configuration for all polytypes (Table 2). The energy differences between C_2 and A dislocation cores range from 0.146 to 0.152 eV Å^{-1}. Overall, the situation is quite similar to silicon, for which C_2 is more stable than A, with an energy difference in the range 0.14–0.16 eV Å^{-1} [20,51]. Core radii and energies are also reported in Table 2. The former quantity is here computed by assuming that all the excess energy in the computational cell due to dislocations is equal to the anisotropic elastic energy [39]. Note that interactions between dislocations, both in the cell and due to periodic boundary conditions, have been taken into account to determine the core radius of a single dislocation. Following another definition of the core radius, now equal to the Burgers vector, the computed dislocation core energies are also reported in Table 2. Comparing the energy-related quantities for the different polytypes, it clearly appears that the differences are very small, and comparable to the level of accuracy of the calculations. Therefore, polytypism has no or negligible influence on the stability properties of dislocations.

4. Peierls stress calculations

The threshold shear strain needed to displace a screw dislocation in the basal plane was first determined for the 4H-SiC polytype. This was done by applying a ε_{zy} deformation to the computational cell, and monitoring the evolution of the structure during relaxation. This method is the simplest one and allows for an accurate determination in agreement with more sophisticated approaches [52,53]. Considering initially the most stable C_2 core, it was found that applying a 10% shear strain did not lead to dislocation displacement. Adding a further 4% did not change the situation. At this point, it is reasonable to consider that 14% is a value large enough to qualify the C_2 as sessile. This point was corroborated by additional interatomic potential calculations, not described here, which showed that for larger shear strains, the C_2 is transforming to a moving A core plus a remaining coordination defect. This situation is comparable to the silicon one, for which it is currently thought that only shuffle dislocations are mobile in the low-temperature/high-stress regime, although they are less stable than glide dislocations [54].

Considering now the A_c configuration, it was found that the structure remains fixed when applying an initial strain of 6.0%. However, at 6.1%, the dislocation becomes unstable and is displaced in the next Peierls valley, here the next hexagonal center, in the basal plane and the $\hat{x}$ direction. The most important displacements during the dislocation migration are obtained for the two rows of atoms between two successive Peierls valleys, the same ones defining the "long" bonds described in the previous section. The sign of the height difference along $\hat{z}$ between the two atomic rows is reversed during the migration, the middle structure being equivalent to a B dislocation core. This mechanism has already been described in detail in the literature [42,52]. To determine the stress σ_{zy} corresponding to the shear strain ε_{zy}, the appropriate elastic modulus has to be calculated. For these orientations it should be equal to $C_{44} = 159$ GPa. Using the second method, with the sheared bulk, $C = 157$ GPa is obtained, in very good agreement with C_{44}. This yields a Peierls stress of 9.5 GPa for the A_c dislocation core in the basal plane of 4H-SiC. For the A_h core, it was found that the dislocation is displaced for a slightly lower value of 6.0%, corresponding to a Peierls stress of 9.4 GPa, the migration mechanism being rigorously the same as for the A_c configuration. It is difficult to estimate whether the small 0.2 GPa difference has a real meaning or is simply indicative of the accuracy of the calculations.

The same procedure was performed for the other 2H and 3C polytypes. Only A configurations were considered, since tests have shown that the C_2 dislocation core is also sessile. For 2H, the calculated threshold shear strain is 6.4% for the A_h structure, the only relevant configuration. The corresponding modulus computed using a 6.4% sheared pristine bulk is 151 GPa, in excellent agreement with the bulk computed $C_{44} = 153$ GPa (Table 1). Then the computed Peierls stress of the A_h dislocation core is 9.6 GPa, quite close to the value obtained for 4H-SiC. In the case of 3C-SiC, the threshold shear strain was determined equal to 5.4%. The sheared bulk calculation yields an associated modulus $C = 165$ GPa. Again, this is in excellent agreement with the value computed using elastic constants, $C = \frac{1}{3}(C_{11} + C_{44} - C_{12}) = 164$ GPa. The Peierls stress for the A_c configuration in 3C-SiC is then 8.9 GPa, thus slightly lower than in hexagonal polytypes. Thus, it is tempting to say that the Peierls stress of non-dissociated screw dislocation increases as a function of the hexagonality of the SiC polytypes. Nevertheless, although the calculated stress range (0.7 GPa) is not negligible, it remains relatively low (at most 8%). It is also interesting to compare the 3C-SiC results with Peierls stress data computed for silicon. First-principles investigations suggested a value of 3.6–4 GPa for the Peierls stress of the screw dislocation in the A configuration [55,20], i.e. 4% of the bulk modulus (100 GPa). In the case of 3C-SiC, the computed value is also exactly 4% of the bulk modulus (220 GPa). Although this may be a coincidence, this suggests a possible scaling effect.

Not that due to the use of periodic boundary conditions, what is considered in calculations is an infinite arrangement of interacting dislocations. When the applied strain is close to the threshold value, the two dislocations in the computational cell can be displaced towards each other, thus changing the interactions. This would lead to an extra force on dislocations, which could artificially increase or decrease the determined Peierls stress. Using elasticity theory, this contribution can be estimated by calculating the interaction energy per unit length along $\hat{z}$ as a function of the displacement x of the dislocations:

$$E = \frac{Kb^2}{2\pi} \sum_{n=-\infty}^{\infty} \sum_{\substack{m=-\infty \\ m+n \text{ is odd}}}^{\infty} \ln \frac{\sqrt{(nd-2x)^2 + (mh)^2}}{r_0} \quad (1)$$

Here, we considered only interactions between dislocations of opposite Burgers vectors, as the only one depending on x. Also we assumed that the dislocation displacement is along the $\hat{x}$ axis. In this equation, d and h are the separations between consecutive dislocations along $\hat{x}$ and $\hat{y}$ respectively, and r_0 the core radius. K is the energy factor, which is $\sqrt{C_{44}C_{66}}$ for hexagonal systems and C_{44} for the cubic one [39]. The force on dislocations is obtained by taking the derivative with respect to x, and the corresponding stress is:

$$\Delta\sigma = -\frac{Kb}{\pi} \sum_{n=-\infty}^{\infty} \sum_{\substack{m=-\infty \\ m+n \text{ is odd}}}^{\infty} \frac{nd-2x}{(nd-2x)^2 + (mh)^2} \quad (2)$$

This stress contribution has been estimated for the computational setup used for the screw dislocation in 4H-SiC. The only unknown quantity is the dislocation displacement x at the critical shear strain, which is likely to be small. An upper bound is $d_0/4, d_0$ being the distance between two Peierls valleys along $\hat{x}$, since it is approximately the inflection point in the Peierls potential [52]. Fig. 4 shows the variation of $\Delta\sigma$ for different x values as a function of the size of the cell. The latter is changed by multiplying d and h by a scaling factor, a value of 1.0 corresponding to the cell dimensions used for the first-principles calculations in this work. As expected, the additional stress is minimal for large cell dimensions or for small x values. For the setup used in this work, $\Delta\sigma$ is positive, thus leading to an underestimation of the calculated Peierls stress. However, the maximum contribution (for $x \simeq d_0/4$) is only 0.09 GPa, which is lower than the stress increment used in the first-principles calculations.

5. Discussion

Microscopy observations revealed that dislocations in the low-temperature/high-stress regime are non-dissociated in SiC [15]. The investigation of core stability reported in this paper indicates that there are only two possible candidates for a non-dissociated screw dislocation: the A core in "shuffle" planes and the C_2 core in "glide" planes. Although C_2 is the lowest-energy configuration, Peierls stress calculations suggested that this core is sessile. These elements indicate that the observed non-dissociated screw dislocations have an A core and are "shuffle" dislocations, like in silicon [54].

As mentioned in the Introduction, there are no available measurements of the Peierls stress in SiC. Nonetheless, a recent investigation of the mechanical properties of 3C-SiC micropillars revealed that ductile deformation by dislocation nucleation could be obtained at room temperature for the lowest diameters, with a corresponding resolved shear stress ranging from 4.9 to 7.3 GPa [56]. There are no further details regarding the nature of the dislocations, but they are likely to be non-dissociated. The measured stresses are of the same order of magnitude as the value of 8.9 GPa computed for 3C-SiC in this work. A likely explanation for the difference is the effect of thermal activation since micropillar deformation was done at room temperature. This allows for a significant reduction of the stress required to displace the dislocation [57]. Another assumption is a possible influence of the polycrystalline nature of the micropillars. Finally, one cannot exclude that the first-principles value is an overestimation of the true Peierls stress due to quantum effects, as recently revealed in metals [58].

Finally, the calculations reported here are useful for discussing cross-slip mechanisms. Since screw dislocations are non-dissociated at low temperature, cross-slip is possible in any planes containing the dislocation line according to continuum elasticity theory. Obviously, one should also consider the crystalline structure of the material. In the case of the cubic polytype, there are two equivalent {111} planes, (111) and $(1\bar{1}1)$, in which the shuffle A_c screw dislocation could move along directions $[1\bar{2}1]$ and [121] respectively (Fig. 3). Peierls stresses for these two slip systems are obviously equal by symmetry. Another slip system could be [101](010), corresponding to the successive transformation of the screw dislocation between A and C configurations. This case was examined for silicon, leading to the conclusion that such a process is not occurring under the sole action of stress [55]. In fact, the A→C transformation requires thermal activation because of a large energy barrier, with a low dependence on the applied stress [59]. Furthermore, once in the C_2 configuration, a dislocation would stop for the same reasons explained above. This slip system is then forbidden for the screw dislocation (marked with the ∥ symbol in Fig. 3). Therefore, in the cubic polytype, the screw dislocation could slip (and cross-slip) in two different planes, making an angle α.

Now the comparison with polytypes 2H and 4H becomes interesting, since hexagonal systems miss the symmetry reported above. Because the atomic arrangements of cubic and hexagonal polytypes are locally similar, one might expect that a screw dislocation could also glide in the plane making an angle α with the basal plane in the case of 2H and 4H, albeit over a distance of the same order as one hexagon. In such a process, the screw dislocation would transform between A_h and A_c configurations, passing through intermediate B structures. The slip direction would change when the screw dislocation is located in an "hexagonal" hexagon, since we assume that the transformation from A to C geometries is not possible. The proposed mechanism is depicted in Fig. 3. The slip system seen at a larger scale would be the prismatic plane $(1\bar{1}00)$ and an average [0001] displacement direction, resulting from the zigzag motion of the dislocation. This scenario has been tested by determining the associated Peierls stress for the 4H polytype. An increasing ε_{zx} deformation was applied, thus shearing the computational cell along the $(1\bar{1}00)$ plane, with either an initial A_c or A_h core

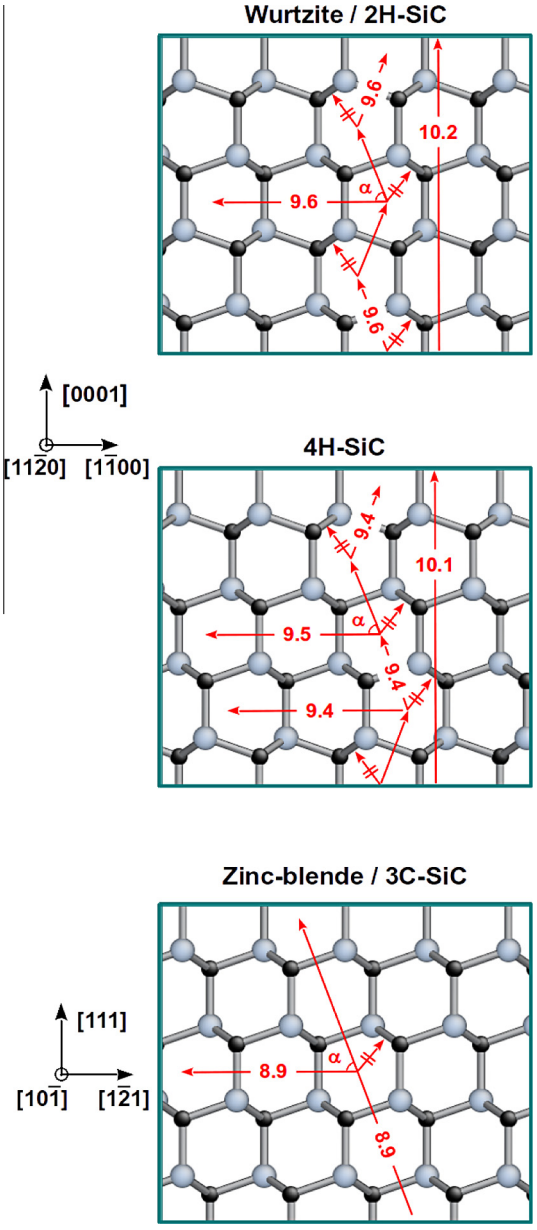

Fig. 3. Similar representation to Fig. 1, showing directions for the movement of a non-dissociated shuffle screw dislocation as well as corresponding computed Peierls stresses in GPa (in red for online version). Dislocations displacement along directions marked with ∥ symbols are forbidden. $\alpha = \arccos(1/3)$ is the supplementary of the angle between two successive Si–C bonds. (For interpretation of the references to colour in this figure caption, the reader is referred to the web version of this article.)

dislocation. In both cases, the dislocation was observed to do a single A→B→A displacement for a shear strain value of 5.3%. Depending on the starting configuration, the final geometry was either A_h or A_c, after displacement in the direction making an angle α with the normal to the basal plane. Applying such a shear strain on a pristine bulk system allows for determining an elastic modulus of 190 GPa, which is slightly lower than the value computed using elastic constants ($C_{66} = 203$ GPa). The Peierls stress required to displace the screw dislocation with the zigzag mechanism, i.e. with an average slip along the [0001] direction,

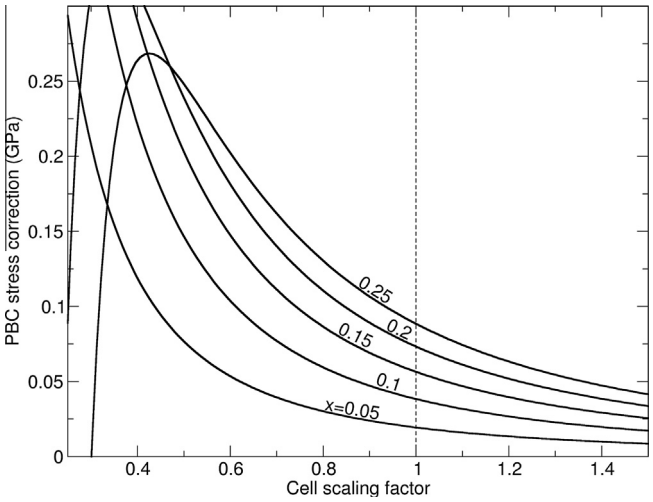

Fig. 4. Stress contribution associated with periodic boundary conditions as a function of the computational cell size (d and h scaled, with h/d constant), for different dislocation displacements x (in unit of d_0).

is then $190 \times 0.053 \simeq 10.1$ GPa. This corresponds to a resolved shear stress of $10.1 \times \cos(90^\circ - \alpha) = 9.5$ GPa for the A→B→A mechanism at the scale of an hexagon, equal to the value of 9.4–9.5 GPa previously computed for the $[1\bar{1}00](0001)$ slip system. With such an excellent agreement, it is straightforward to determine a Peierls stress of 10.2 GPa for the same mechanism in the case of 2H-SiC, using the data calculated for the A_h core dislocation displacement in the basal plane. The Peierls stresses for dislocation displacement in the prismatic plane are then 6% higher than in the basal plane in 2H and 4H polytypes. This is in clear contrast with the cubic polytype for which cross-slip between (111) and $(1\bar{1}1)$ planes can occur for the same stress. It is not certain that such a small stress difference could be evidenced experimentally. However, one may hope that future observations could show cross-slip events with angles between slip planes which would be different between 3C on the one side and 2H and 4H on the other side. This would confirm the zigzag motion of the screw dislocation for an average displacement along the prismatic plane, predicted in this work for hexagonal polytypes.

6. Summary

The stability and mobility of non-dissociated screw dislocations in 4H, 2H and 3C polytypes of SiC have been studied using first-principles calculations. In this material, it has in fact been shown that plasticity properties at low temperature greatly depend on these extended defects, for which very little is known. These investigations lead to the following conclusions:

- Only two dislocation cores are stable. One is centered in the middle of an hexagon (Fig. 1), in "shuffle" planes (A). The second one, C_2, is characterized by a reconstruction along the dislocation line, and is located in

"glide" planes. It is also energetically more stable than the former one. The situation is similar for the three polytypes, and also to what is known for silicon.

- Peierls stress calculations indicate that the most stable C_2 dislocation core is sessile, while the Peierls stress related to the A core is in the range 8.9–9.6 GPa, depending on the polytype. Then the A core is predicted to be the one observed in microscopy experiments.
- There is overall a negligible influence of polytypism on the quantities characterizing the stability and mobility of a non-dissociated screw dislocation. However, it is predicted that slip planes will be different in cubic and hexagonal polytypes, due to the differences in crystal symmetry. Possible slip planes in 3C-SiC are {111} planes, while in hexagonal systems, basal and prismatic planes are involved. In the latter case, the prismatic displacement would result from a zigzag motion of the dislocation.

Acknowledgements

This work was partially supported by the program NEEDS "Materials for nuclear energy" (CNRS, CEA, EDF, AREVA). It also pertains to the French Government program "Investissements d'Avenir" (LABEX INTERACTIFS, reference ANR-11-LABX-0017-01). Prof. J.-L. Demenet is gratefully acknowledged for fruitful discussions.

References

[1] Harris G, editor. Properties of silicon carbide, INSPEC, London. Institution of Electrical Engineers; 1995.
[2] Katoh Y, Snead L, H. Jr C, Hasegawa A, Kohyama A, Riccardi B, Hegeman H. Current status and critical issues for development of sic composites for fusion applications. J Nucl Mater (Part A) 2007;367370:659–71. <http://www.sciencedirect.com/science/article/pii/S0022311507004497>.
[3] Hinoki T, Katoh Y, Snead L, Jung H-C, Ozawa K, Katsui H, et al. Silicon carbide and silicon carbide composites for fusion reactor application. Mater Trans 2013;54(4):472.
[4] Oliveros A, Guiseppi-Elie A, Saddow S. Silicon carbide: a versatile material for biosensor applications. Biomed Microdevices 2013;15:353.
[5] Pirouz P. Some aspects of the structural, mechanical and electronic properties of sic. In: Ghetta V, Gorse D, Mazire D, Pontikis V, editors. Materials issues for generation IV systems. NATO science for peace and security series B: physics and biophysics. Netherlands: Springer; 2008. p. 327–50.
[6] Sitch PK, Jones R, Öberg S, Heggie MI. Ab initio investigation of the dislocation structure and activation energy for dislocation motion in silicon carbide. Phys Rev B 1995;52(7):4951.
[7] Blumenau AT, Fall CJ, Jones R, Heggie MI, Briddon PR, Frauenheim T, et al. Straight and kinked 90° partial dislocations in diamond and 3C-SiC. J Phys: Condens Matter 2002;14:12741.
[8] Blumenau AT, Fall CJ, Jones R, Öberg S, Frauenheim T, Briddon PR. Structure and motion of basal dislocations in silicon carbide. Phys Rev B 2003;68:174108.
[9] Chen H-P, Kalia RK, Nakano A, Vashishta P, Szlufarska I. Multimillion-atom nanoindentation simulation of crystalline silicon carbide: orientation dependence and anisotropic pileup. J. Appl. Phys. 2007;102(6). http://dx.doi.org/10.1063/1.2781324. <http://scitation.aip.org/content/aip/journal/jap/102/6/10.1063/1.2781324>.
[10] Laref A. Structural properties of partial dislocation in 3C-SiC. Mater Lett 2011;65(2122):3301–4. http://dx.doi.org/10.1016/j.matlet.2011.07.007. <http://www.sciencedirect.com/science/article/pii/S0167577X11007762>.
[11] Zhang H. The properties of shockley partials in crystalline cubic silicon carbide (3C-SiC): core width and Peierls stress. Physica B 2011;406(67):1323–5. http://dx.doi.org/10.1016/j.physb.2011.01.025.
[12] Ohno Y, Yonenaga I, Miyao K, Maeda K, Tsuchida H. In-situ transmission electron microscopy of partial-dislocation glide in 4h-sic under electron radiation. Appl Phys Lett 2012;101(4):042102. http://dx.doi.org/10.1063/1.4737938. <http://scitation.aip.org/content/aip/journal/apl/101/4/10.1063/1.4737938>.
[13] Lara A, Castillo-Rodríguez M, Muñoz A, Domínguez-Rodríguez A. Dislocation microstructure of 4hsic single crystals plastically deformed around the transition temperature. J Eur. Ceram Soc 2012;32(2):495–502. http://dx.doi.org/10.1016/j.jeurceramsoc.2011.08.016. <http://www.sciencedirect.com/science/article/pii/S0955221911004183>.
[14] Sun Y, Izumi S, Sakai S, Yagi K, uki Nagasawa H. Core element effects on dislocation nucleation in 3C-SiC: Reaction path way analysis. Comput Mater Sci 2013;79(0):216. http://dx.doi.org/10.1016/j.commatsci.2013.05.055. <http://www.sciencedirect.com/science/article/pii/S0927025613003364>.
[15] Demenet J-L, Amer M, Tromas C, Eyidi D, Rabier J. Dislocations in 4H- and 3C-SiC single crystals in the brittle regime. Phys Stat Sol (c) 2013;10(1):64–7.
[16] Demenet J-L, Milhet X, Rabier J. Tem observations of the coexistence of perfect and dissociated dislocations in sic under high stress. Phys Stat Sol (c) 2005;2(6):1987.
[17] Mussi A, Demenet J-L, Rabier J. Tem study of defects generated in 4H-Sic by microindentations on the prismatic plane. Philos Mag Lett 2006;86(9):561.
[18] Pizzagalli L, Beauchamp P, Rabier J. Stability and core structure of undissociated screw dislocations in group iv materials investigated by means of atomistic calculations. J Phys: Condens Matter 2002;14:12681.
[19] Pizzagalli L, Beauchamp P, Rabier J. Stability of undissociated screw dislocations in zinc-blende covalent materials from first principle simulations. Europhys Lett 2005;72(3):410.
[20] Wang C-Z, Li J, Ho K-M, Yip S. Undissociated screw dislocation in Si: glide or shuffle set? Appl Phys Lett 2006;89:051910.
[21] Pizzagalli L, Godet J, Guénolé J, Brochard S. Dislocation cores in silicon: new aspects from numerical simulations. J Phys Conf Ser 2012;281:012002. http://dx.doi.org/10.1016/j.physleta.2013.04.038.
[22] Rabier J, Montagne A, Demenet JL, Michler J, Ghisleni R. Silicon micropillars: high stress plasticity. Phys Stat Sol (c) 2013;10(1):11. http://dx.doi.org/10.1002/pssc.201200546.
[23] Schulz H, Thiemann K. Structure parameters and polarity of the wurtzite type compounds Sic2H and zno. Solid State Commun 1979;32(9):783–5. http://dx.doi.org/10.1016/0038-1098(79)90754-3. <http://www.sciencedirect.com/science/article/pii/0038109879907543>.
[24] Silicon carbide (sic), lattice parameters, thermal expansion. In: Madelung O, Rössler U, Schulz M, editors. Group IV elements, IV-IV and III-V compounds. Part b – electronic, transport, optical and other properties, Landolt–Börnstein – group III condensed matter, vol. 41A1b. Berlin, Heidelberg: Springer; 2002:p. 1–11.
[25] Kamitani K, Grimsditch M, Nipko JC, Loong C-K, Okada M, Kimura I. The elastic constants of silicon carbide: a brillouin-scattering study of 4H and 6H Sic single crystals. J Appl Phys 1997;82(6):3152–4.
[26] Djemia P, Roussigné Y, Dirras G, Jackson K. Elastic properties of β-sic films by brillouin light scattering. J Appl Phys 2004;95(5):2324.
[27] Lambrecht WRL, Segall B, Methfessel M, van Schilfgaarde M. Calculated elastic constants and deformation potentials of cubic sic. Phys Rev B 1991;44:3685–94. http://dx.doi.org/10.1103/PhysRevB.44.3685. <http://link.aps.org/doi/10.1103/PhysRevB.44.3685>.

[28] Sarasamak K, Limpijumnong S, Lambrecht WRL. Pressure-dependent elastic constants and sound velocities of wurtzite sic, gan, inn, zno, and cdse, and their relation to the high-pressure phase transition: a first-principles study. Phys Rev B 2010;82:035201.
[29] Iuga M, Steinle-Neumann G, Meinhardt J. Ab-initio simulation of elastic constants for some ceramic materials. Eur Phys J B 2007;58(2):127–33. <http://dx.doi.org/10.1140/epjb/e2007-00209-1>.
[30] Karch K, Pavone P, Windl W, Schütt O, Strauch D. Ab initio calculation of structural and lattice-dynamical properties of silicon carbide. Phys Rev B 1994;50:17054–63. http://dx.doi.org/10.1103/PhysRevB.50.17054. <http://link.aps.org/doi/10.1103/PhysRevB.50.17054>.
[31] Hohenberg P, Kohn W. Inhomogeneous electron gas. Phys Rev 1964;136(3B):B864.
[32] Kohn W, Sham LJ. Self-consistent equations including exchange and correlation effects. Phys Rev 1965;140(4A):A1133.
[33] Giannozzi P, Baroni S, Bonini N, Calandra M, Car R, Cavazzoni C, et al. Quantum espresso: a modular and open-source software project for quantum simulations of materials. J Phys: Condens Matter 2009;21(39):395502. <http://www.quantum-espresso.org>.
[34] Perdew JP, Burke K, Ernzerhof M. Generalized gradient approximation made simple. Phys Rev Lett 1996;77(18):3865.
[35] Vanderbilt D. Soft self-consistent pseudopotentials in a generalized eigenvalue formalism. Phys Rev B 1990;41(11):7892.
[36] Bigger JRK, McInnes DA, Sutton AP, Payne MC, Stich I, King-Smith RD, et al. Atomic and electronic structures of the 90° partial dislocation in silicon. Phys Rev Lett 1992;69(15):2224.
[37] Lehto N, Öberg S. Effects of dislocation interactions: application to the period-doubled core of the 90° partial in silicon. Phys Rev Lett 1998;80(25):5568.
[38] Bulatov V, Cai W. Computer simulations of dislocations. Oxford series on materials modelling. New York: Oxford University Press; 2006.
[39] Hirth JP, Lothe J. Theory of dislocations. New York: Wiley; 1982.
[40] Monkhorst HJ, Pack JD. Special points for brillouin-zone integrations. Phys Rev B 1976;13(12):5188.
[41] Béré A, Serra A. Atomic structure of dislocation cores in gan. Phys Rev B 2002;65:205323.
[42] Pizzagalli L, Beauchamp P, Rabier J. Undissociated screw dislocations in silicon: calculations of core structure and energy. Philos Mag A 2003;83:1191.
[43] Belabbas I, Nouet G, Komninou P. Atomic core configurations of the $\vec{a}$-screw basal dislocation in wurtzite gan. J Cryst Growth 2007;300:212.
[44] Hornstra J. Dislocations in the diamond lattice. J Phys Chem Solids 1958;5:129.
[45] Rabier J, Pizzagalli L, Demenet J-L. Dislocations in silicon at high stress. In: Kubin L, Hirth JP, editors. Dislocation in solids, vol. 16. Elsevier; 2010. p. 47 [Chapter 93].
[46] Arias TA, Joannopoulos JD. Ab initio theory of dislocations: from close-range spontaneous annihilation to the long-range continuum limit. Phys Rev Lett 1994;73(5):680.
[47] Miyata M, Fujiwara T. Ab initio calculation of Peierls stress in silicon. Phys Rev B 2001;63:45206.
[48] Blumenau AT, Heggie MI, Fall CJ, Jones R, Frauenheim T. Dislocations in diamond: core structures and energies. Phys Rev B 2002;65:205205.
[49] Celli V. Screw dislocation in crystals with diamond structure. J Phys Chem Solids 1961;19(1/2):100.
[50] Koizumi H, Kamimura Y, Suzuki T. Core structure of a screw dislocation in a diamond-like structure. Philos Mag A 2000;80(3):609.
[51] Pizzagalli L, Demenet JL, Rabier J. Theoretical study of pressure effect on the dislocation core properties in semiconductors. Phys Rev B 2009;79:045203.
[52] Pizzagalli L, Beauchamp P, Jónsson H. Calculations of dislocation mobility using nudged elastic band method and first principles dft calculations. Philos Mag 2008;88(1):91.
[53] Rodney D, Proville L. Stress-dependent Peierls potential: Influence on kink-pair activation. Phys Rev B 2009;79:094108.
[54] Pizzagalli L, Beauchamp P. Dislocation motion in silicon: the shuffle-glide controversy revisited. Philos Mag Lett 2008;88(6):421.
[55] Pizzagalli L, Beauchamp P. First principles determination of the Peierls stress of the shuffle screw dislocation in silicon. Philos Mag Lett 2004;84(11):729.
[56] Shin C, Jin H-H, Kim W-J, Park J-Y. Mechanical properties and deformation of cubic silicon carbide micropillars in compression at room temperature. J Am Chem Soc 2012;95(9):2944.
[57] Pizzagalli L, Pedersen A, Arnaldsson A, Jónsson H, Beauchamp P. Theoretical study of kinks on screw dislocation in silicon. Phys Rev B 2008;77:064106.
[58] Proville L, Rodney D, Marinica M-C. Quantum effect on thermally activated glide of dislocations. Nat Mater 2012;11:845.
[59] Guénolé J, Godet J, Pizzagalli L. Determination of activation parameters for the core transformation of the screw dislocation in silicon. Modell Simul Mater Sci Eng 2010;18:065001.